CHAPTER-3

Teak sawdust derived mesoporous carbon-supported gamma alumina synthesis for crystal violet dye removal from wastewater: Characterization and Removal study

Chapter 3: Teak sawdust derived mesoporous carbon-supported gamma alumina synthesis for crystal violet dye removal from wastewater: Characterization and Removal study:

3.1. Surface Topography of Adsorbent (SEM Analysis):

A scanning electron microscope (SEM) was used to evaluate the synthesized adsorbent's surface appearance and structure. Gamma mesoporous alumina ornamentation on the MAC surface is uniformly evaluated using the MAC@Al image. The surface of MAC at 700 °C exhibits a tiny pore creation during synthesis, with uniform distribution of gamma alumina following hydrothermal composition, as seen in **Figure 3. 1. (a) and (b).** When the activated carbon was fully formed, the surface of the micropores was transformed into meso and macro pore sizes, and the meso-gamma alumina was evenly distributed across the surface of the MAC. Since teak wood sawdust is used as a precursor for MAC fabrication, **Figure 3.1. (e) and (f)** for MAC@Al demonstrates the cylindrical pore surface development by decorating its surface with gamma alumina [165]. For MAC@Al, **Figure 3.1. (c) and (d)** also demonstrate the development of cubic and cylindrical pore types with some surface aggregation of mesoporous gamma-alumina. During the pyrolysis and activation processes for the creation of MAC, the uniqueness of the teak sawdust may be preserved [166]. The porous surface of the MAC@Al adsorbent burst and filled with colour within 30 minutes of the crystal violet dye sticking to it, as seen in **Fig. 3.3. Figure 3.4** shows the EDAX and MAC@Al mapping following crystal violet dye adsorption. The detection of nitrogen and chlorine in EDAX further validated the adsorption of crystal violet dye on the adsorbent MAC@Al. **Figure 3.2.** displays a SEM image of raw teak sawdust-based bare activated carbon (BAC) that has been heated to 700 °C. The surface properties of the sawdust-based BAC adsorbent are shown in **Fig. 3.2. (a)** for BAC.

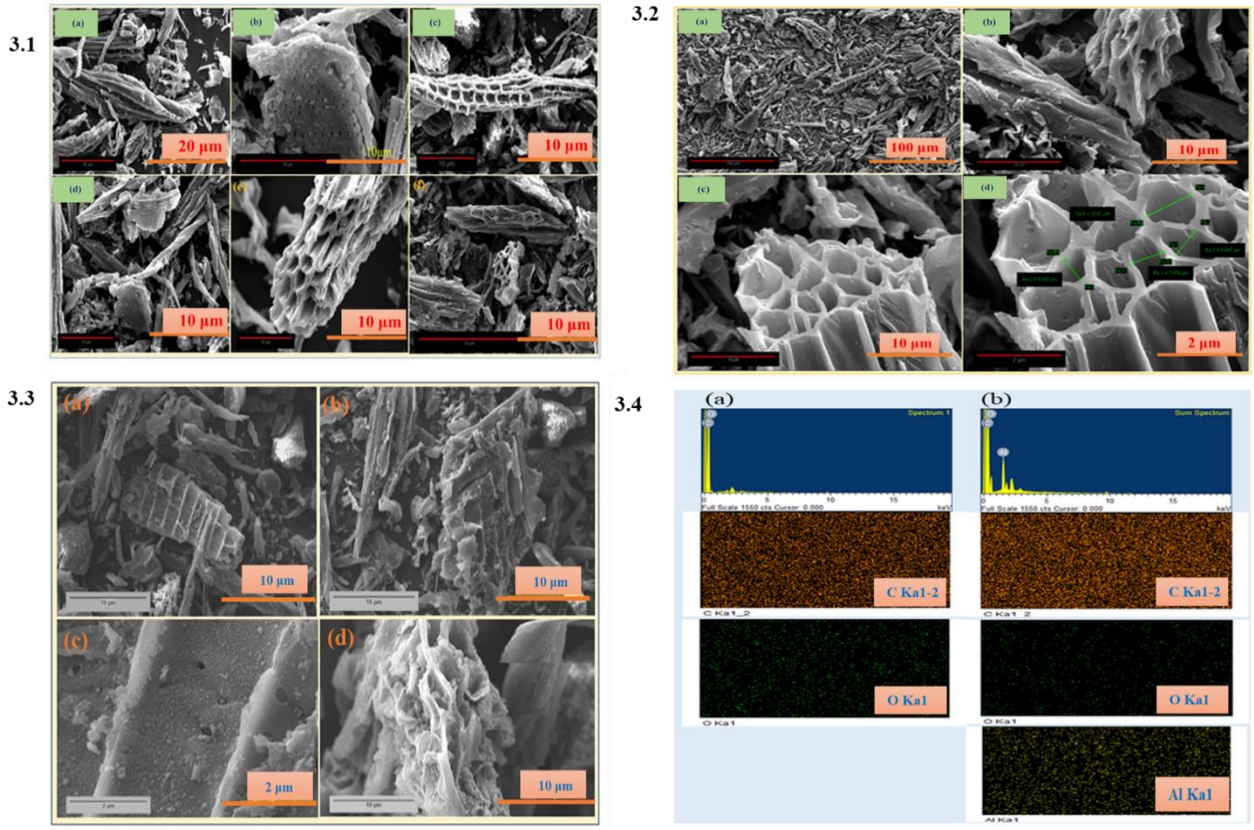

Figure 3-1 3.1. MAC@Al before adsorption, **3.2.** BAC before adsorption, **3.3.** MAC@Al after CV dye adsorption, and **3.4. (a)** BAC and **(b)** MAC@Al EDAX and Elemental mappings.

This displays the wide-pore surface picture. The BAC adsorbent had less pore size formation because of the disorganized carbon that was created when the organic components in sawdust broke down and filled the pores [167]. On the porous surface of BAC, the adsorption of crystal violet dye is lower than that of MAC@Al because the surface pore structures have become larger after activation. A possible explanation for the high adsorption removal of crystal violet effluent is the surface decorating of MAC by γ-mesoporous alumina, which could raise the composite's surface porosity. As was previously said in the synthesis section for figuring out the influence of mesopores on gamma alumina, surface-decorated BAC@Al were synthesized to demonstrate this. It was discovered that, in comparison to BAC, the crystal violet dye effluent adsorption reached its maximum at a dye concentration of 40 mg/L in 30 minutes. **Figure 3.4. (a)-(b)** analysed and reported the EDAX and elemental mapping of the synthesized BAC and MAC@Al adsorbent's existing C, O, and Al elements.

3.2. XRD, FTIR, BET and Raman Analysis of the Adsorbent:

The produced gamma-alumina, MAC, BAC, MAC@Al, and BAC@Al adsorbent powder X-ray diffractograms is displayed in **Figure 3-2 (a).** The HR X-ray diffraction device (Rigaku Miniflex CuKα of.154 nm radiation of 30 mA and 40 kV) was used to analyses the X-ray diffraction for each sample. For disordered and graphitized glass-like carbon in BAC and MAC, respectively, the planes (002) and (100) are described by the peak diffraction at around 23.9° and 43.5° [168]. The diffraction angles at 66.5°, 45.5°, and 37.5° are equivalent to the gamma-alumina reflections at (440), (400), and (331) [169]. Both MAC@Al and BAC@Al displayed diffraction at 18.78°, 23.9°, 26.68°, 40.50°, 45.5°, and 66.5° following hydrothermal preparation, which corresponded to the (111), (002), (112), (222), (400), and (440) planes [170,171]. Both disordered carbon and gamma-alumina are present in these planes. The moisture concentration of BAC@Al causes Al $(OH)_3$ diffraction in the (112) planes [172].Hence, the synthesis of MAC@Al and BAC@Al adsorbents has been done.

In case of FTIR analysis, the synthesized adsorbents' surface chemical functionalization was assessed using a Fourier Transform Infra-Red (FTIR) spectrophotometer (Model: Nicolet iS5 Company: THERMO Electron Scientific Instruments LLC). **Figure 3-2 (b).** displays the synthesized adsorbents' FTIR spectra. A peak at 3440 cm^{-1} was found in each of the adsorbents, showing that the existence of moisture caused the -OH bond to expand and vibrate [173]. The C-H stretching vibration is evident as a peak at 2970 and 2920 cm^{-1} in all of the adsorbents that leave gamma-alumina. The existence of C=O and C=C functional groups in synthesized carbonaceous materials is shown by the peaks at 1700 and 1590 cm^{-1} [174]. The peaks at 1640 and 1400 cm^{-1} in gamma-alumina, respectively, indicate the presence of modest Al-O and Al-OH bending vibrations [171]. The existence of mild C-O bending vibration on the surface of mesoporous carbon is indicated by the peak at 1080–1100 cm^{-1} in carbonaceous adsorbents (except for gamma-alumina) [175]. The presence of the Al-O and Al-O-Al vibrations is confirmed by the broad extending peak at 810 cm^{-1} and 580 cm^{-1}. All carbonaceous adsorbents (BAC, MAC, BAC@Al, and MAC@Al) have tiny out-of-plane vibration peaks at 880 cm^{-1} that indicate the existence of the C-H functional group. A tiny

out-of-plane bending -OH was measured at 476 cm^{-1} in the BAC adsorbent [168,176]. The presence of C-H bending vibration in mesoporous carbon adsorbent is indicated by the peak in the MAC adsorbent near 820, 756 cm^{-1}. Since there is no bond disappearance (shifting of position indicating the aromatic tertiary amine bond interaction with MAC@Al), the FTIR spectrum of crystal violet dye adsorbed on the surface of MAC@Al for 30 minutes by 40-ppm concentration is displayed in **Figure 3-2(b).** This indicates that there is a slight variation in the wavenumber position of the MAC@Al adsorbent due to physical or ion exchange phenomenon [103,177].

Characterizing the porous texture of activated carbon is necessary to understand the activation's effect and the activating agent's ($ZnCl_2$) influence on activated carbon utilized in biomass. For this, the BET (Brunauer-Emmett-Teller) and BJH (Barrett–Joyner–Halenda) instrumental techniques were used to assess the surface porosity and surface area of ZnCl2-based Mesoporous Activated Carbon (MAC) and γ-alumina-decorated MAC (MAC@Al). At 77K, the N_2 adsorption-desorption isotherm was discovered. The resultant isotherm diagram displays type IV hysteresis [112]. The pore and surface area plots of MAC and MAC@Al adsorbent, respectively, are shown in **Figure 3-2 (c)-(d)**, which also indicates the isotherm plots that demonstrate the production of mesoporosity in these two adsorbents. The surface area and porosity table are provided in **Table 3-2-1**.. In figure 3-2 (c), MAC adsorbent shows open loop it may be due to irreversible adsorption gas or it can be because of pore nature of materials due to slow diffusion or mass transfer limitation. One other cause may be the instrumental error due to moisture.

In addition to other information regarding the crystalline carbon structure, the degree of order and crystallinity of carbon materials were ascertained using Raman spectroscopy. It is used to analyze the crystalline structure of carbon, with the primary focus of the MAC MAC@Al adsorbent being the G band (Graphitic 1580 cm^{-1}) and the D band (Disorder 1360 cm^{-1}) [112,178]. According to calculations, the I_D/I_G ratios for MAC and MAC@Al are 1.40 and

1.12, respectively, indicating that there are fewer defects in the MAC adsorbent than in MAC@Al [179]. **Figure 3-2 (e)** represents the Raman spectrum of the adsorbent

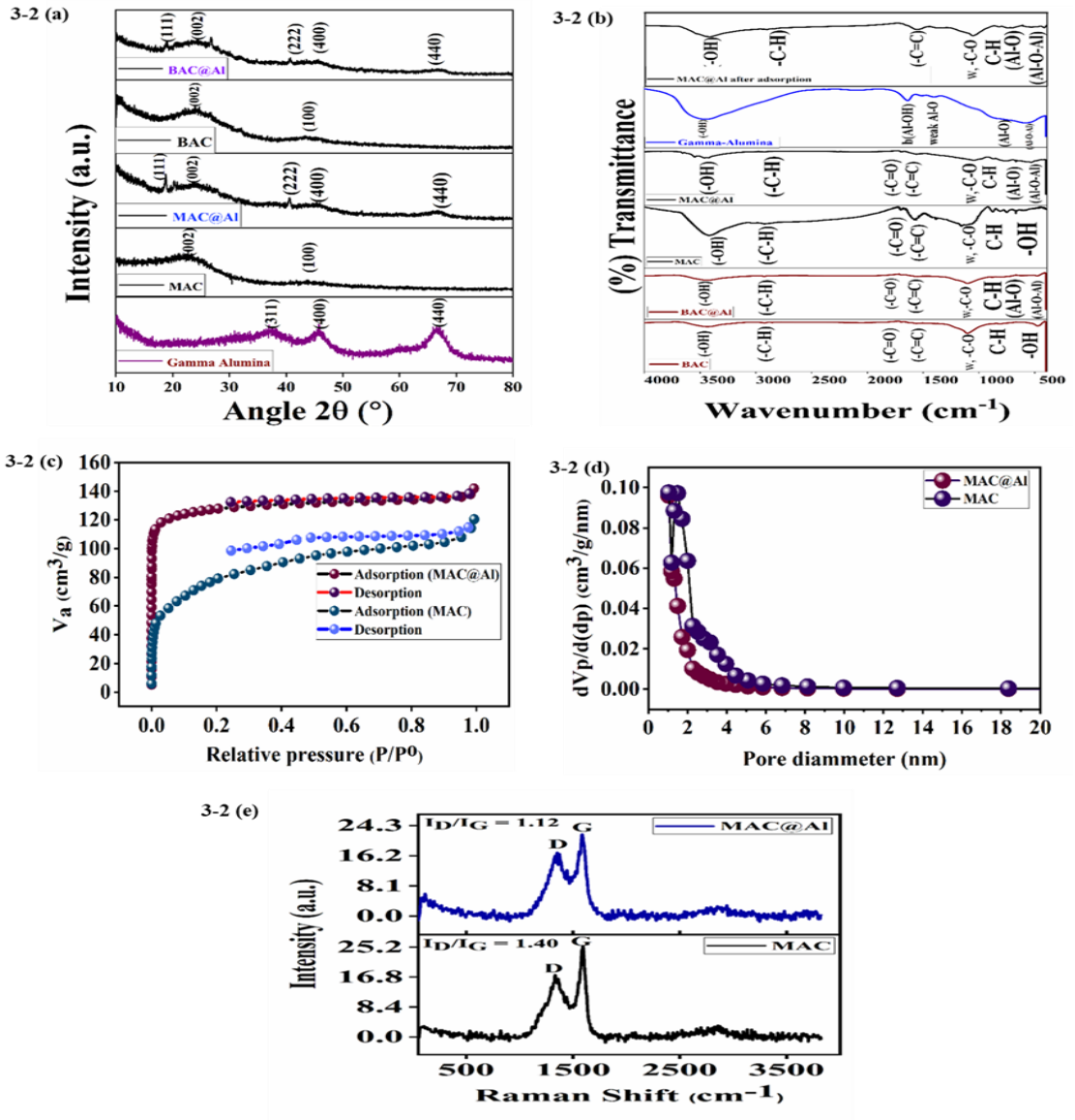

Figure 3-2 (a) XRD all adsorbents, (b) FTIR of all adsorbents and after CV dye adsorption, (c) BET isotherm, (d) BJH pore diameter plot, and (e) Raman Spectrum of MAC and MAC@Al, respectively

Adsorbents	BET SSA (m^2/g)	Mean Pore Diameter (nm)	Total Pore Volume (cm^3/g)
MAC	271	2.70	**0.183**
MAC@Al	**393**	**2.21**	**0.218**

Table 3- 2- 1 Surface Properties of MAC and MAC@Al adsorbents

3.3. X-ray Photoelectron Analysis of the Adsorbents:

Using X-ray photoelectron spectroscopy (XPS) Model: K-Alpha, Company: Thermo Fisher Scientific, the X-ray photoelectron spectra of adsorbed and desorbed crystal violet dye on the MAC@Al surface were assessed. The results are displayed in **Figure. 3-3 (a), (c), (e), (g), (i) (adsorbed) and (b), (d), (f), and (h)** (desorbed) respectively. 1N CH_3COOH aqueous solution was used for dye desorption, and 0.1M NaOH aqueous solution was used for neutralization. The N 1s XPS **Fig. 3-3 (i)** peak is seen with C 1s, O 1s, and Al 2p when crystal violet dye is adsorbed on the MAC@Al surface. The N 1s peak at 400.08 eV has also been seen with the survey peak **Fig. 3-3 (a).** The existence of C-Al, C-C, C-N/C-O, and -C=O at 283.3 eV, 284.28 eV, 285.5 eV, and 287.5 eV with sp^2 and sp^3 hybridization properties, respectively, was discovered by deconvolution of the C 1s peak in the adsorbed MAC@Al adsorbent [180–183]. The existence of O=C / Al O(OH) and O-Al bonds was detected at 531.5 eV and 529.98 eV in the O 1s spectra of adsorbed dye on MAC@Al adsorbent[184,185]. Al-Al and Al_2O_3/Al-O Bonds are formed when the Al 2p of adsorbed dye on MAC@Al deconvolutes at 73.5 eV and 74.8 eV, respectively [186,187]. Once crystal violet dye has been adsorbed onto the MAC@Al adsorbent surface, the N 1s XPS spectra are visible. This demonstrates that Ph-NR_2 and Ph=N^+-R_2 (Ph = Phenyl) bonds are present at 399.3 eV and 401.68 eV, respectively, due to the existence of N in these forms in crystal violet dye [188]. The MAC@Al adsorbent based on desorbed crystal violet dye is also examined using an XPS instrument, and the C 1s, O 1s, and Al 2p were detected during the analysis. C-Al, C=C/C-C, C-O, and C=O were detected in the C 1s spectra at 283.8 eV, 284.8 eV, 285.5, and 288.1 (± 0.5 eV shifting), respectively [189]. **Figure 3-3 (f)** displays the O 1s XPS spectra of the desorbed dye, revealing the similar presence of the O-Al and O-C/Al O (OH) bond at 530.8

eV and 531.5 eV with slight shifting. Likewise, the Al 2p XPS spectra show a slight (± 0.1eV) shift in the desorbed MAC@Al adsorbent's binding energy. The successful surface decorating of gamma alumina on mesoporous activated carbon is demonstrated by the bond energies at 73.5 and 74.8 eV in **Figure 3-3 (h)**. During analysis, this presence is confirmed by the C-Al bond in **Figure 3-3 (d)**. The inclusion of the groups increased the carbon materials' wettability and favoured their interaction with aqueous pollutants, which boosted their adsorption capacity [190]. The adsorption of crystal violet dye on the surface of the MAC@Al adsorbent is confirmed by the existence of C-Al, C-N, and displaced O-Al bonds in the figures above. Additionally, the Ph-NR_2 and Ph=N^+-R_2 (Ph = Phenyl) bonds at 399.3 eV and 401.68 eV demonstrate that the MAC@Al adsorbent successfully adsorbed the crystal violet dye. Overall, the adsorbed and desorbed wastewater pollutants on the adsorbent surface can be verified using X-ray photoelectron spectroscopy based on their oxidation state and binding energy, which were verified in this instance of crystal violet adsorption.

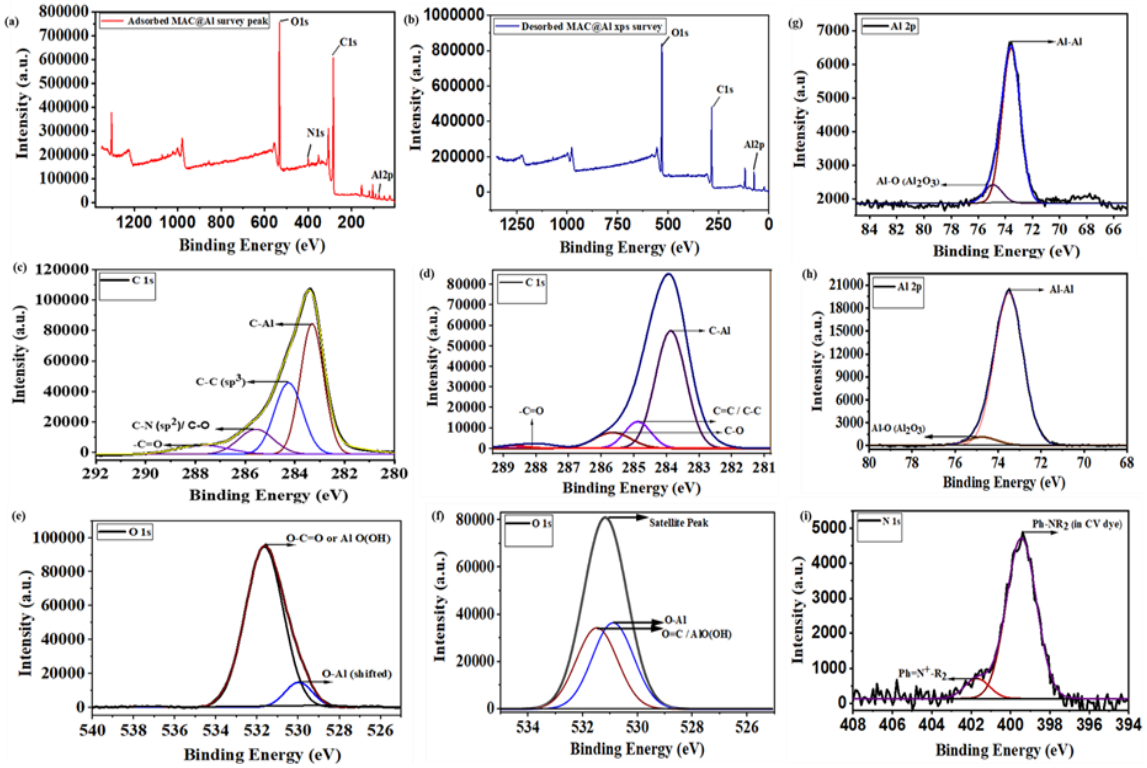

Figure 3-3. XPS spectra of MAC@Al adsorbed CV dye **(a), (c), (e), (g), (i),** and MAC@Al adsorbent: **(b), (d), (f) and (h).**

3.4. Adsorption Study of Crystal Violet Dye:

3.4.1. Initial Concentration and Time Impact Analysis:

An initial concentration of crystal violet dye ranging from 20 to 80 ppm was prepared in order to evaluate the effect of crystal violet dye concentration during adsorption. As the initial dye concentration rose, the percentage of crystal violet dye clearance fell. It could be as a result of insufficient active surface sites of the adsorbent to absorb the crystal violet dye [191]. For 30 minutes, the reaction was conducted at a temperature of 298 K. The availability of the active areas on the sorbent surface explains why q_e increases as C_i increases in **Figure 3-4-1-(a)** [192]. The analysis for each adsorbent's equilibrium adsorption period revealed that it was 30 minutes and the time needed to remove crystal violet dye are shown in **Figure 3-4-1 (b)-(f),** The dye removal investigation was conducted using 0.01g of catalytic MAC@Al adsorbent at 298K temperature for 2, 5, 7, 10, and 30 minutes. To keep the solution's pH neutral, four stocks of crystal violet dye (20, 40, 60, and 80 ppm) were made using 0.1M HCl and NaOH solution. Following the adsorption method, the residual concentration of each stock before and after was determined by using a UV-VIS spectrophotometer to create a calibration plot shown in **Figure 3-4-1 (h)** for crystal violet at $\lambda_{max.}$= 590 nm. Because surface-active areas on the adsorbent are initially covered, the removal of crystal violet dye diminishes as the initial dye concentration rises, as shown **in Fig. 3-4-1 (b)**. **Fig. 3-4-1 (c)** displays the removal adsorption capability of different doses of crystal violet dye [193]. To determine the efficacy of MAC@Al adsorbent over BAC and BAC@Al adsorbents, a relative time study was conducted for the removal of crystal violet dye. For this, a solution containing 20, 40, 60, and 80 ppm of crystal violet dye was prepared by fixing the 0.01g dose of BAC, BAC@Al, and MAC@Al adsorbents. At a temperature of 298 K, the reaction involving each adsorbent was carried out for 2, 5, 7, 10, and 30 minutes. For the removal research of each adsorbent, the pH of the dye solution was maintained at a neutral level. The only objective of these comparative reaction tests was to verify the effective adsorption of crystal violet dye over time using various adsorbents. Based on this, an adsorption reaction was carried out, and **Fig. 3-4-1 (d), (f), and (g)** show the removal percentage versus time graph that was

plotted. The elimination of a 40-ppm concentration of crystal violet dye was assessed using the BAC, BAC@Al, and MAC @Al adsorbents in combination. It is shown in **Fig. 3-4-1 (e)**. It was determined from this plot that MAC@Al adsorbent removes more crystal violet dye than BAC and BAC@Al adsorbent. It might be due to the MAC@Al adsorbent's surface topography. The removal capability of the adsorbate has been enhanced by the mesoporous γ-Al_2O_3 modification of MAC. It is evident from the study on the removal of 40 parts per million (ppm) of crystal violet dye that the removal efficacy rises when mesoporous γ-Al_2O_3 is added to the BAC. This further proves that the original adsorbent surface was successfully altered

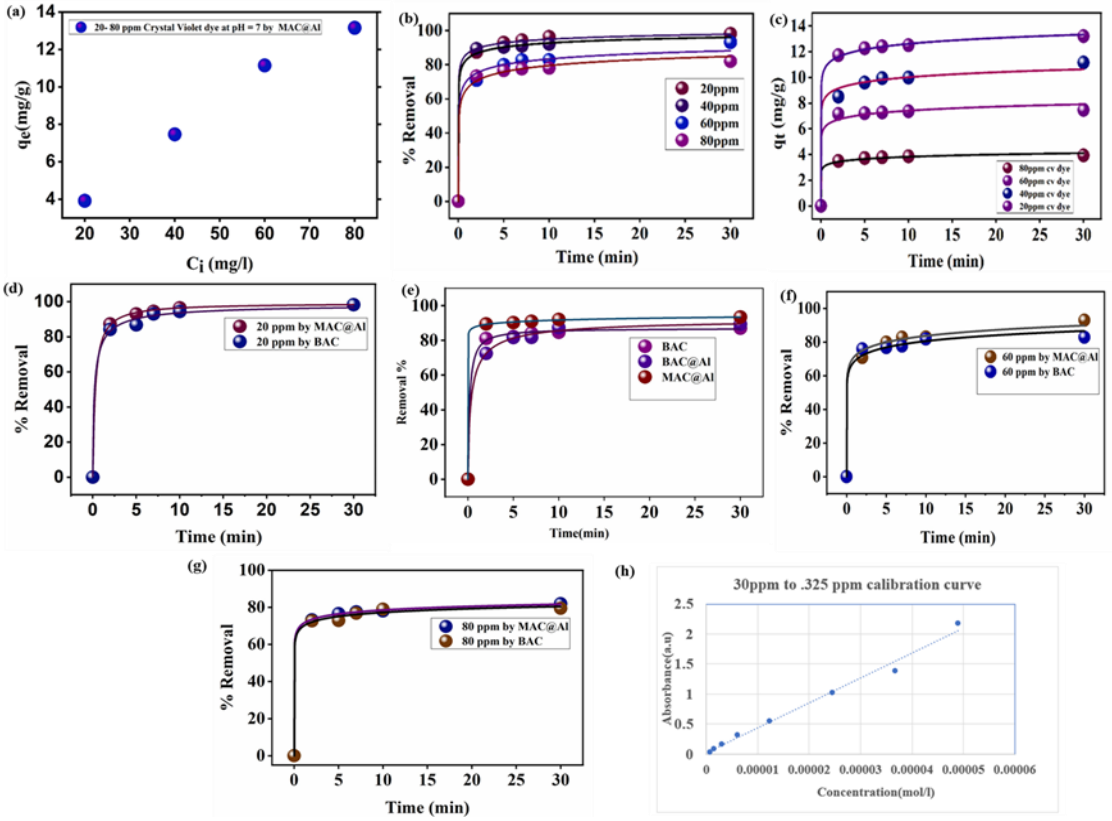

Figure. 3-4-1 (a) initial concentration vs equilibrium adsorption capacity plot from 20-80 ppm CV dye at neutral pH 298 K **(b)** Plot of crystal violet dye removal percentage versus time at pH=7 for 20, 40, 60 and 80 ppm from 2-30 minutes by MAC@Al **(c)** Plot of crystal violet dye's adsorption capacity (mg/g) with time variation at pH=7 for 20, 40, 60 and 80 ppm from 2-30 minutes by MAC@Al **(d)** Graph of Time against percentage elimination of

20-ppm crystal violet dye at pH=7 at 298 K by MAC@Al and BAC **(e)** Graph of Time against percentage elimination of 40-ppm crystal violet dye at pH=7 at 298 K by MAC@Al, BAC@Al and BAC **(f)** Graph of Time against percentage elimination of 60-ppm crystal violet dye at pH=7 at 298 K by MAC@Al and BAC **(g)** Graph of Time against percentage elimination of 80-ppm crystal violet dye at pH=7 at 298 K by MAC@Al and BAC **(h)** Calibration plot of CV dye from 0.325 ppm to 30 ppm from UV-Vis spectrophotometer at 590 nm wavelength.

3.4.2. Impact of pH, pHzpc on removal and dose study of adsorbent:

Previous research has shown that the initial pH has a significant impact on surface loading and the degree of ionization of functional groups on the adsorbent surface, making it one of the key parameters influencing efficiency and adsorption capacity. MAC@Al adsorbent was utilized to examine the impacts of acidity, basicity, and neutralization on the removal of crystal violet dye by measuring the pH values of the effluent [194]. Different pH values of 4, 5, 7, 8, and 9 were used to create a 40 ppm Crystal Violet dye solution. 0.01g of MAC@Al adsorbent was added to each of the different pH dye solutions, and the mixture was kept at 298 K for 30 minutes in an incubator water bath shaker (Narang Pvt.ltd) spinning at 250 rpm. Reduced availability of dissolved oxygen, which is essential for aquatic species, is another way that high pH values may harm aquatic life. For this reason, all optimization studies were run at pH 7, with the maximum removal occurring at pH 9. The study found that eliminating contaminants requires a pH of 6 to 8, with a pH of 6 to 8 being optimal. The study concluded that controlling pH levels is necessary for effective contaminant removal from water [195]. After 30 minutes of adsorption, the amount of crystal violet dye left at λmax. 590 nm was measured using a UV-VIS spectrophotometer. **Figure 3-4-2 (a)** shows the absorbance versus wavelength curve of various pH crystal violet dye solutions following adsorption. The ideal pH for the removal of crystal violet dye was found to be 99.38 % at pH 9 after research into the pH variation of dye effluents. **Fig. 3-4-2 (b)** explained. During these investigations, the percentage of crystal violet removal increased as the pH in an alkaline solution rose. This behaviour resulted from higher dye sorption caused by the stronger electrostatic interaction

between cationic dye molecules and negative MAC@Al surfaces charged with OH^- [196]. The pHzpc method was used to convolute the adsorbent material's zero-point surface charge. **Figure 3-4-2 (c)** plots the starting pH against ΔpH. In this work, 10 mL of NaCl was utilized for the investigation, which has already been documented in the literature, and 100 mg of MAC@Al adsorbent was utilized for the adsorption of 0.01 M of NaCl solution [197]. The MAC@Al adsorbent's pHzpc was found to be 7.27, which is extremely close to the neutral pH of water and wastewater. According to the results of pH and pHzpc, the MAC@Al adsorbent's surface has a negative charge for pH > pHzpc and a positive charge at pH< pHzpc. The adsorption of crystal violet dye increased as the pH was raised from acidic to basic conditions. The adsorbent's negative surface and the dye's cationic surface (pH>pHzpc) caused the dye to be removed more readily. The scenario may be caused by a strong gravitational pull and a decrease in the repulsive force between the adsorbent MAC@Al surface and the crystal violet dye [198]. Because H^+ ions in aqueous solution compete with dye colour for localization on active adsorbent sites, CV's reduced efficacy in acidic circumstances using both adsorbents may be caused by this [199].

A dosage analysis for crystal violet dye effluent using a synthetic MAC@Al adsorbent was carried out. A dose variation of 2, 4, 6, and 10 mg of MAC@Al adsorbent was used to achieve a 40-ppm concentration of crystal violet dye. The reaction was run at 298K and neutral pH for 30 minutes. Crystal violet dye effluents can be effectively removed with a 4 mg dosage of the MAC@Al adsorbent. The residual concentration after the adsorption of crystal violet dye at different MAC@Al doses was investigated using a UV-VIS spectrophotometer. Plotting the removal per cent and adsorption capacity of crystal violet dye at time t against the adsorbent dose (mg) allowed researchers to examine these variables. **Figure 3-4-2 (d)** shows the absorbance versus wavelength plot for the remaining crystal violet dye following adsorption. The 4 mg dosage of MAC@Al adsorbent was found to be effective in **Figure 3-4-2 (e)**. With an adsorption capacity of 18.7 mg/g, the adsorption percentage removal for a 4 mg dosage of MAC@Al adsorbent for 40 ppm crystal violet dye

was equivalent to 93.45%. The adsorption capacity at time t, or 30 minutes, is depicted by the q_t in **Figure 3-4-2 (e)**.

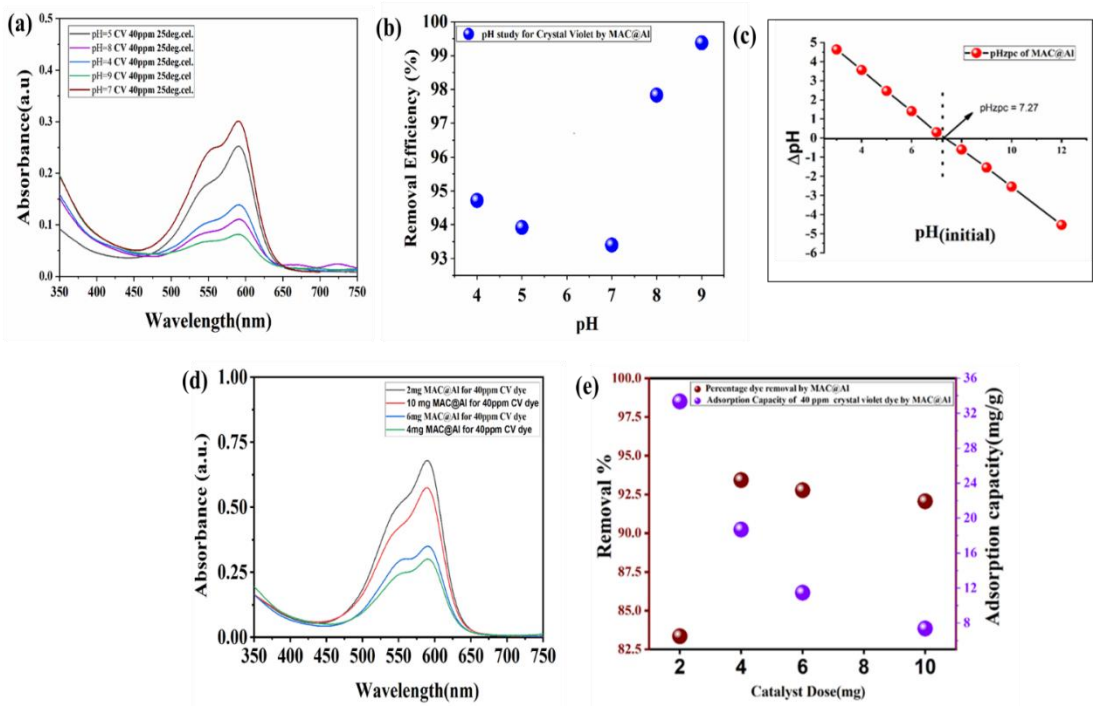

Figure 3-4-2 (a) Wavelength versus Absorbance plot for adsorbed crystal violet 40-ppm at 298K dye at various pH of MAC@Al adsorbent, **(b)** Removal graph of crystal violet dyes effluents at pH = 4, 5, 7 8 and 9 for 40-ppm at 298K within 30 minutes using MAC@Al adsorbent, **(c)** pHzpc study of MAC@Al adsorbent from pH 3-12 at 298 K for 24h, **(d)** Wavelength versus Absorbance plot for different Dose of MAC@Al adsorbed by 40-ppm crystal violet dye at 298 K for 30 min, **(e)** Removal percentage and adsorption capacity graph for crystal violet dye adsorbed by various doses of MAC@Al adsorbent 2-10 mg at pH=7 for 30 min at 298 K temperatures.

3.4.3. Interference Study of Hazarodus Metal Salts in CV Dye Removal:

The effects of several metal salts on the remediation of crystal violet dye effluent were examined. 40 ppm crystal violet dye was used in 40 and 80 ppm solutions of different metal salts for this experimental study. For the interference investigation, these metal salt solutions were made over the allowable limits [200,201]. To examine the interferences and evaluate the

effectiveness of the dye removal procedure, solutions of metal salts and crystal violet dye were made in deionized water at concentrations of 80 and 40 ppm and 40 with 40 ppm, respectively. The following metal salts, including chromium (III) nitrate 9 H_2O, anhydrous $FeCl_3$, $MgCl_2$, $CaCl_2$, and Na_3AsO_4, were used for the interference research. In the removal investigation, 0.01g of MAC@Al adsorbent was used for 2, 5, 7, 10, and 30 minutes at 298K temperature and neutral pH. **Figure 3-4-3 (b)** displays the comparison removal graph of 40 ppm crystal violet dye with 40 and 80 ppm all metal salt solution combined and individually done. The interference study of metal salts on crystal violet dye effluents using MAC@Al adsorbent for 80-40 ppm concentration separately revealed that the removal efficiency of Ca^{2+}, Mg^{2+}, Cr^{3+}, and As^{5+} metal salts was lower than that of 40-ppm crystal violet dye, but it was somewhat higher for Fe^{3+}. It might be because iron (III) salts on the MAC@Al adsorbent surface have a binding property. Comparing Fe^{3+} to 40-ppm crystal violet dye removal, which was 94 % effective, the removal effectiveness increased to 96.5 %. **Figure 3-4-3 (a)** illustrates how various metal salts interfere with the removal of 40 ppm crystal violet dye. In all other metal salt examples, it had decreased somewhat, from 94 % to 84 %. These metal salts may cover the adsorbent's surface sites, which prevents the MAC@Al adsorbent from efficiently adsorbing the crystal violet dye in solution. However, the adsorption effectiveness was not significantly reduced during these interferences, which further indicates the existence of partially covered active sites on the adsorbent material's surface. The interferences of all 40 and 80 ppm combination metal salts are shown in **Fig. 3-4-3 (b)**, which also demonstrates how the MAC@Al adsorbent reduced the percentage of crystal violet dye eliminated as compared to 40 ppm crystal violet dye. All things considered, this interference study may adequately explain how water-based inorganic metal

contaminants, which are typically prevalent in rivers, lakes, groundwater, and industrial coastal areas, affect the adsorption of crystal violet dye [202,203].

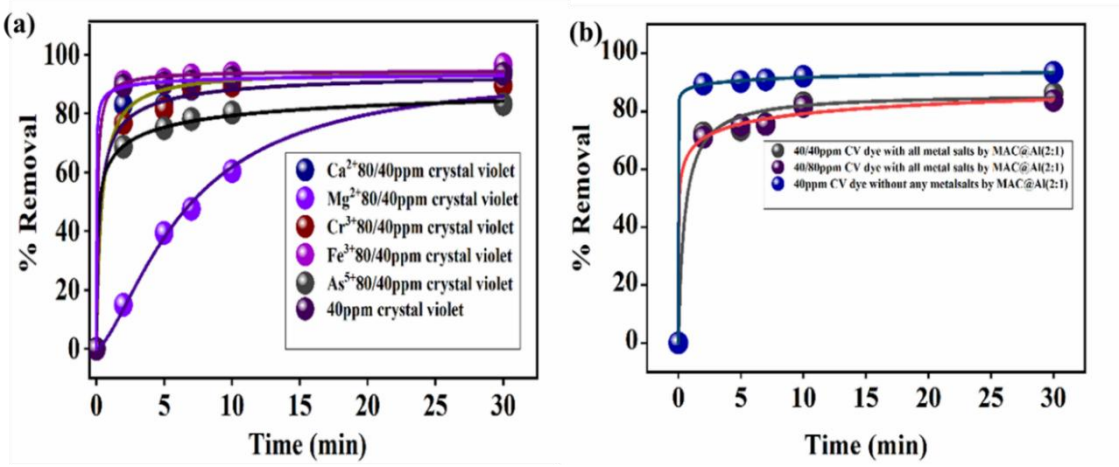

Figure 3-4-3. (a) Plot of percentage crystal violet dye elimination versus time for each metal salt individually at pH=7 from 2-30min. at 298 K. **(b)** Plot of time versus percentage removal of crystal violet dye with all metal salts interference combinedly at pH=7 from 2-30 min at 298 K.

3.4.4. Crystal Violet Dye Removal Study Using the River Ganga Water:

Ganga wastewater was gathered from the Varanasi Assi Ghat area in order to investigate the impact of river water on the removal of Crystal Violet dye using MAC@Al adsorbent. For the study, a sample is taken five meters into the river. The Ganga effluent had been filtered to eliminate the trash and other contaminants. After additional measurements, the wastewater's pH was found to be 8.3. This is the pH of the river water that was collected. In order to investigate the dye removal within 30 minutes at pH 8.3, a 40-ppm crystal violet dye stock was created using 20 mL of river water. The 40-ppm crystal violet dye duration vs removal percentage graph is displayed in **Figure 3-4-4 (a)**. When comparing Ganga Water to deionized water, the elimination of crystal violet is a little higher, as seen in Figure **3-4-4 (b)**. After 30 minutes, the proportion of crystal violet dye removed was 98.21 %. It was found that the pH of 8.3 adhered to the previously determined pH study limits for the elimination of crystal violet dye.

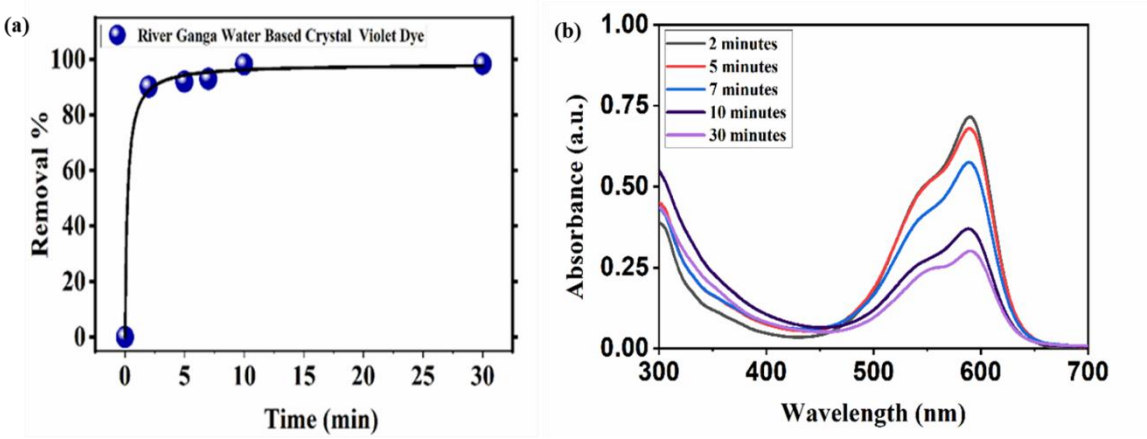

Figure 3-4-4 (a) The 40-ppm crystal violet dye (Using Ganga Water) Percentage Removal from 2-30 minutes at pH=7 at 298 K using MAC@Al adsorbent. **(b)** UV-VIS Wavelength versus absorbance graph of adsorbed crystal violet dye from 2-30 minutes at 590 nm.

3.4.5. Adsorption Kinetic Modelling:

Important information on the equilibrium state of the operation can be obtained from studies on the kinetic behaviour of the adsorption process. Numerous models, such as the Elovich model, intra-particle diffusion model, pseudo-first-order (PFO), and pseudo-second-order (PSO) models, can be used to analyse the kinetic behaviour. The PFO and PSO models, which are commonly used to determine the type of physical or chemical interactions that exist between the contaminating ions and the adsorbent surface, were used in this work.

The kinetics of Crystal Violet dye on the MAC@Al adsorbent surface was investigated using pseudo-first and second order (PFO and PSO) kinetic models. The analysis was conducted at 298K using stocks of 40 ppm of Crystal Violet dye concentration. The fluctuation in the adsorbate's concentration and elimination rate over time determines the rate of change of the adsorbate at a specific reaction time, according to pseudo-first-order kinetic [155,156,159]. Plotting the kinetics data of PFO and PSO, which are shown in **Figure 3-4-5 (a) and (b)**, allowed for the analysis and study of both models for the removal of crystal violet dye. The Pseudo Second Order model is the best-fitting kinetic model in the instance of crystal violet dye removal, which was investigated at 298 K using MAC@Al adsorbent. This indicates that the MAC@Al adsorbent surface experienced chemical adsorption of crystal violet. Equations

(12) and (14) were used for PFO and PSO analysis. **Figure 3-4-5 (c)** presents the results of the MAC@Al adsorbent by Elovich model adsorption kinetics study at 20, 40, 60, and 80 ppm crystal violet dye. Table 3-4-5-1 provides the slope and intercept values that were obtained experimentally, along with the adjacent R^2 value and standard error, with the sum of square error. The study's R^2 values were not even near unity 1, unlike the Freundlich adsorption isotherm (0.99), indicating that the dye's physical adsorption predominates in this investigation. Equation (16) was used for Elovich kinetic analysis. Equation (17) was used for intra-particle diffusion analysis of crystal violet dye on the surface of MAC@Al adsorbent at 298 K temperature. **Figure 3-4-5 (d)** shows the $t^{0.5}$ vs q_t plot for this model and all the data for this model is given in **Table 3-4-5-1**.

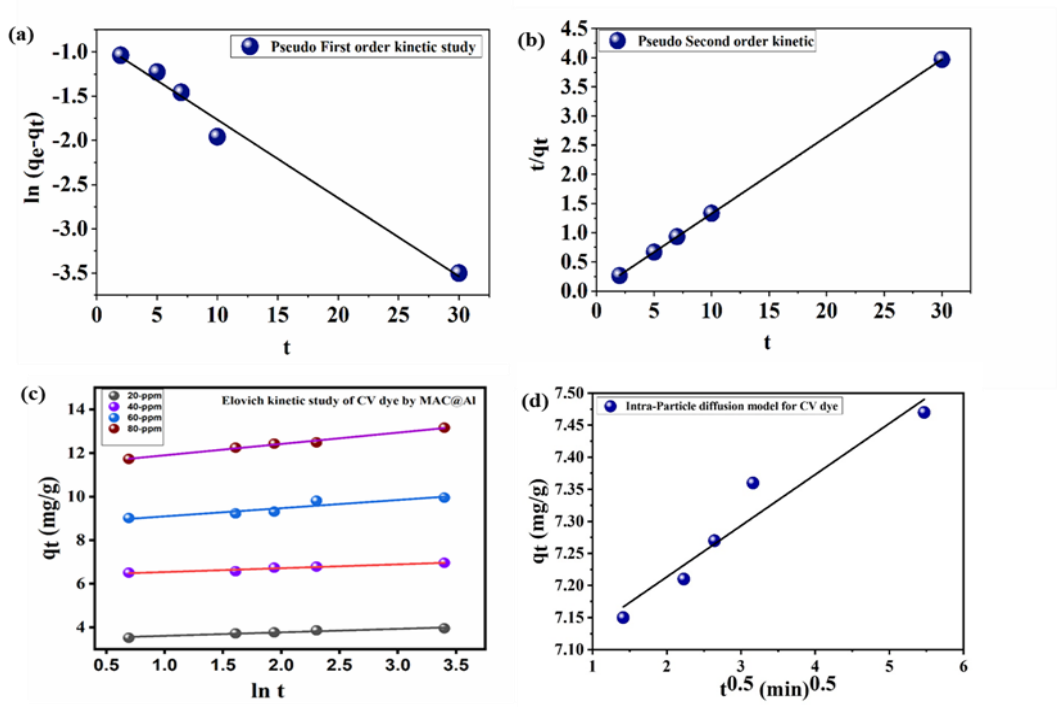

Figure 3-4-5 (a) Pseudo First Order kinetics, (b) Pseudo Second Order Kinetics, (c) Linearly fitted Elovich regression model for 20-80 ppm CV dye by MAC@Al adsorbent from 2,5,7, 10 and 30 min at 298K, (d) Intra-particle diffusion Model.

R^2 values in the case of PFO and PSO are 0.987 and 0.99, respectively. the rate constant value in PFO k_1 is 0.08 $min^{-1,}$ with experimental q_e 1.08 mg/g and for PSO, the k_2 is 2.79 g/mg min, with q_e(experimental) = 7.5 mg/g at 298 K and neutral pH.

Parameters notations	For the Elovich model	For the Intra-Particle diffusion model	R^2
β (20 ppm)	6.28		0.93
β (40 ppm)	5.68		0.92
β (60 ppm)	2.70		0.82
β (80 ppm)	1.92		0.98
k_{diff} (40 ppm)		0.0797	0.935
C (40 ppm)		7.05 (mg/g)	

Table 3-4-5-1 Elovich and Intraparticle diffusion model constant values. The standard error in the above kinetics is below 0.1.

Overall, these kinetic models, the pseudo-second-order kinetics, are best fitted, confirming the adsorption kinetics nature between crystal violet dye and MAC@Al adsorbent. Since the adjacent sum of squares is low enough as compared to the PSO model means the diffusion phenomenon is not fully processed in the role of adsorption of crystal violet from wastewater. 40-ppm CV dye was assessed in the Intra-particle model through which the constant C value came to about 7.05 mg/g, confirming the loading capacity of CV dye by the pore portion of the adsorbent.

3.4.6. Isotherm Study for Crystal Violet Dye Removal:

The Freundlich, Langmuir, Dubinin-Radushkevich, and Temkin model isotherm for crystal violet dye was assessed. The Separation factor used in the Langmuir model is given by the equation

$$R_L = \frac{1}{1+K_L C_i} \quad \text{..... (19)}$$

The equilibrium parameter (R_L), also known as the separation factor, is a dimensionless constant described by the following relationship. This parameter can be used to predict or calculate the sorbent-sorbate affinity. In this instance, the starting concentration is C_i, and the Langmuir constant is represented by K_L. The ideal adsorption value for R_L is between 0 and 1. According to **Figure 3-4-6-(a) and (b)**, the separation factor (RL) for linear form at an 80-ppm concentration of crystal violet dye is 0.081, indicating that the MAC@Al adsorbent

surface has favourable crystal violet dye adsorption. According to the linear regression Langmuir isotherm, 14.8 mg/g has the maximum adsorption capability. **Figure 3-4-6 (c) and (d)** show the non-linear and linear graphs for the elimination of crystal violet dye using MAC@Al adsorbent. It's evident from the above linear and non-linear Freundlich isotherm plot that the wastewater system's crystal violet dye removal process is multilayer in nature. In contrast to the Langmuir adsorption isotherm, the Freundlich isotherm provides a good description of the coefficient R^2 value of 0.99. 0.5, or the 1/n value derived from the plot above, is favourable for the adsorption of crystal violet dye from the wastewater system and falls between 0 and 1 [204–206].

In order to consider the influence of the porous structure of MAC@Al adsorbents, the Dubinin-Radushkevich isotherm model was examined [152]. The Dubinin-Radushkevich isotherm model is commonly utilized to identify any physical or chemical reactions that take place throughout the sorption process. In Chapter 2, the relevant linear equation is shown.

The experimental data are least well-fitted by the D-R model. The mean free energy of absorption, E, or the change in free energy when one mole of an ion is carried from infinity in solution to the surface of a solid, can be calculated using the following formula.

$$E = 1/\sqrt{2k_d} \quad \text{..... (20)}$$

Chemisorption reaction is thought to be responsible for the sorption process if E is between 8 and 16 kJ/mol; if E is less than 8 kJ/mol, the sorption process is thought to be physical. In this instance, the MAC@Al adsorbent is being used in the crystal violet dye removal investigation. The E value is less than 8 kJ/mol, indicating physical adsorption. Figure 3-4-6 (e) shows the D-R model plots. The Temkin isotherm model states that a uniform distribution of binding energies up to a maximum binding energy defines adsorption, and that the adsorption heat of all molecules decreases linearly as the adsorbent surface is covered more.

All of the constants were calculated empirically using the equation in Chapter 2. **Figure 3-4-6 (f)** shows the Temkin model plot.

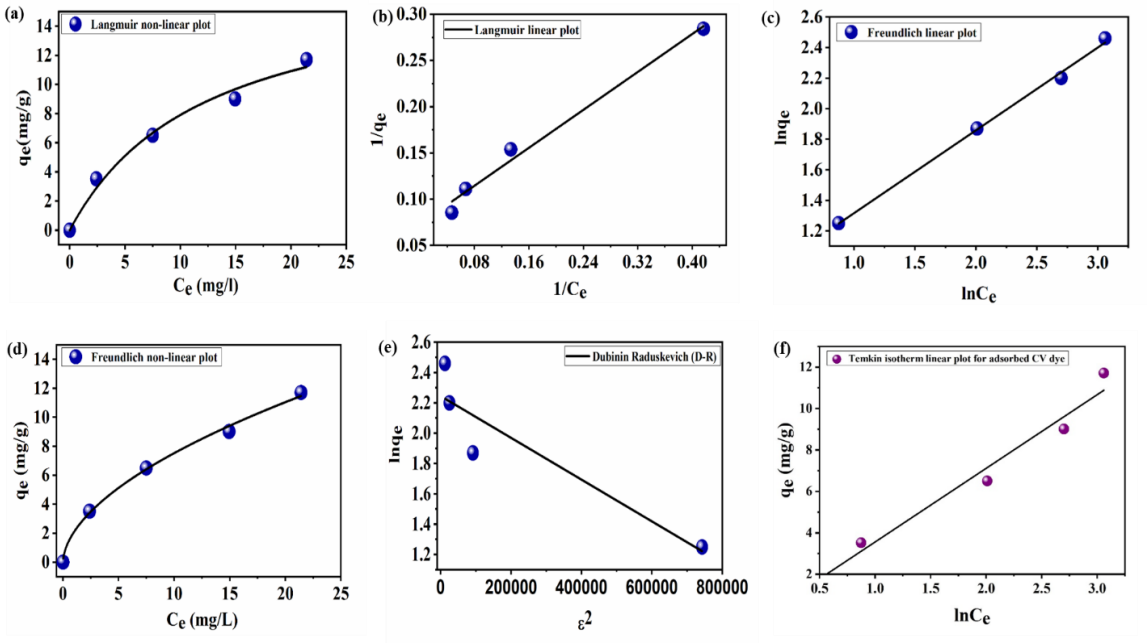

Figure 3-4-6 (a) Langmuir Non-Linear model, **(b)** Langmuir Linear Model, **(c)** Freundlich Non-linear Model, **(d)** Freundlich Linear Model, **(e)** D-R model isotherm, and **(f)** Temkin Isotherm Model.

All the isotherms' models after study showed that the Freundlich isotherm best fitted for the crystal violet dye removal. All isotherm data are tabulated in Table 3-4-6-1 below. In all the isotherms, the standard error was below 0.5, and it has been proven that adsorption of CV dye is physically happening. The comparison of MAC@Al adsorbent with other adsorbents in the literature that have already been used for the removal of crystal violet dye is displayed in Table 3-4-6-2 below. This research gap revealed that the MAC@Al adsorbent is significantly more effective at removing crystal violet dye than the synthesized adsorbent.

Langmuir (linear)	Langmuir (non-linear)	Freundlich (linear)	Freundlich (non-linear)	Dubinin-Radushkevich	Temkin Isotherm
K_L = 0.14 L/g	Ka = 0.08 L/g	K_F = 5.91 L/g	K_F = 2.91 L/g	K_C = 1.3× 10^{-6}	B = 3.35 (mg/g)
q_m = 13.5 mg/g	q_m = 14.8 mg/g	$\frac{1}{n}$ = 0.54	$\frac{1}{n}$ = 0.5	q_m = 9.43 mg/g	A_T = 1.005 (L/g)
R^2 = 0.986	R^2 = 0.981	R^2 = 0.99	R^2 = 0.99	R^2 = 0.786	R^2 = 0.975
T = 298 K	T = 298 K	T = 298 K	T = 298 K	T = 298 K	T = 298 K
pH = 7	pH = 7	pH = 7	pH = 7	pH = 7	pH = 7
R_L = 0.081 between 0 -1 (favourable)				E < 8 kJ/mol	-
Standard Error = 0.00931	Standard Error = 2.73	Standard Error = 0.0461	Standard Error = 0.2236	Standard Error = 0.1489	Standard Error = 0.597
Sum of Square Error (SSE) = 0.0234	Sum of Square (SSE) = 83.9	Sum of Square = 0.818	Sum of Square = 83.9	Sum of Square = 0.818	Sum of Square = 83.98

Table 3-4-6-1 Various Isotherm parameters constant data for Crystal Violet Adsorption on MAC@Al at temperatures 298 K.

3.4.7. Thermodynamics and Regeneration Analysis:

The elimination of crystal violet dye via thermodynamics was investigated at different temperatures (298, 303, 308, and 318 K). By graphing lnK_c vs. 1/T, the Van't Hoff formula was used to calculate the Gibbs free energy (ΔG), enthalpy (ΔH), and entropy (ΔS). **Figure 3-4-7 (a)** shows the Vant Hoff graph for crystal violet dye shown at various temperatures using equation 21. which were employed to determine the values of ΔH and ΔS. The calculation of the thermodynamic term makes use of the Gibbs equation below.

$$\ln K_c = \frac{\Delta S}{R} - \frac{\Delta H}{RT} \quad \text{..... (21)}$$

It is computed by dividing the adsorption capacity at equilibrium, q_e, by the equilibrium concentration of dye, C_e, at each temperature. R is the universal gas constant (8.314 J mol-1 K^{-1}), and K_c, which is dimensionless, is the distribution coefficient constant at constant

temperature. The negative values of ΔH show that adsorption is exothermic and that physical adsorption is possible. The adsorption of crystal violet dye on MAC@Al adsorbent was very favourable, as indicated by the negative values of (ΔG). A decrease in randomness on the MAC@Al surface following the removal of crystal violet dye is indicated by the negative value of ΔS. The thermodynamic parameters are shown in **Table 3-4-7-1.** Research on regeneration and recovery is the field that has to be examined. Adsorbents such as fly ash can be revitalized by chemical, thermal, solvent, and biological processes. An aqueous solution of 1N CH_3COOH was used to desorb the 40-ppm crystal violet dye. Batch mode MAC@Al adsorbent desorption was investigated for one hour at 298 K and 250 rpm. Deionised water and a 0.1M NaOH aqueous solution were used to clean the adsorbent. Its adsorption performance decreased after fourth and fifth cycle is due to filling nonremoved dyes solution inside the pore of MAC@Al and there may be the chance of loss of active sites and surface chemistry changes. When sodium hydroxide solution is being used for regeneration, the waste may be saline water and may contain organic dye contamination.

S.No.	Adsorbent	Adsorption Capacity (mg/g)	References
1.	$CaFe_2O_4$	0.750	[207]
2.	Avocado Pear-Activated Carbon	3.325	[92]
3.	Polyvinylidene fluoride (PVDF) electro-spun membrane	3.84	[208]
4.	Millettia thoningii seed pods activated carbon	7.5	[209]
5.	Flower-based activated carbon	2.69	[210]
6.	Carbon Nanotube	2.615	[211]
7.	Chitosan /AC	12.50	[90]
8.	Cellulose Triacetate	9.11	[212]
9.	Activated carbon	7.513	[213]
10.	**MAC@Al**	**14.8**	**This Work**

Table 3-4-6-2 A comparison table of the research gaps for the adsorption of Crystal Violet dye using different suitable adsorbents and produced MAC@Al.

The amount of dye that underwent desorption was measured using a UV-VIS spectrophotometer, and the desorption efficiency was calculated using the equation from Chapter 2. **Figure 3-4-7 (b)** shows the regeneration removal plot of crystal violet by MAC@Al adsorbent. There might be some commercial activated carbon, which may have a lower or higher adsorption capacity and removal efficiency, like sunflower-derived mesoporous carbon and mesoporous carbon fabrics for CV dye removal.

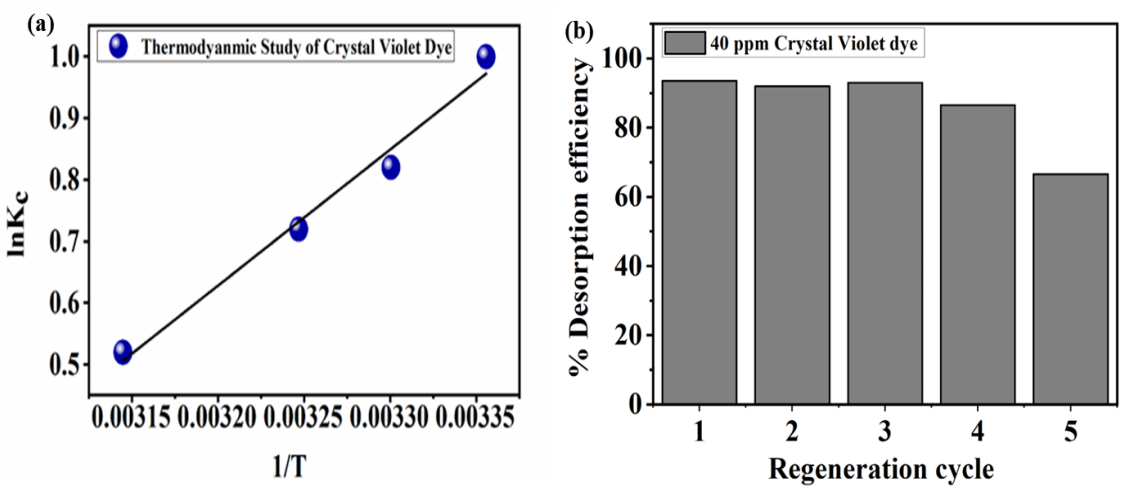

Figure 3-4-7 (a) Van't Hoff plot for crystal violet dye at temperatures 298, 303, 308 and 318 K, pH=7, 200 rpm and time 30 minutes, and **(b)** Reusability of MAC@Al adsorbent for Crystal Violet Removal using 1N CH_3COOH for 40-ppm at pH = 7 within 30 minutes

Temperature (K)	ΔG (kJ/mol)	ΔH (kJ/mol)	ΔS (kJ/K mol)
298	-2.57	-18.36	-0.053
303	-2.31		
308	-2.03		
318	-1.50		

Table 3-4-7-1: All constant experimental values after thermodynamic analysis

From the above table, it is confirmed that adsorption is taking place exothermically, because of negative values of enthalpy and entropy, respectively. the process is continuous at all four temperatures, and it decreases as the temperature increases.

3.4.8. Adsorption Mechanism Analysis:

Crystal violet dye, a cationic dye by nature, can be absorbed by an adsorbent's anionic surface. Following adsorption, crystal violet dye was subjected to FTIR measurement, as illustrated in Figure 3-2 (b). The MAC@Al adsorbent's physical adsorption nature onto their surface is demonstrated by (b), which shows a small shifting of wave numbers with some peak disappearances around 1700 cm^{-1}. The interaction between the tertiary amine group (CV dye) and -OH (MAC@Al) (functionality on the adsorbent surface) is further demonstrated by the change in the wavenumber of the -OH peak upon adsorption of CV dye. Another potential contact might be electrostatic, or between the amine nitrogen and the Al-O bond in MAC@Al, as a result of the FTIR spectrum's wave number changing. The hydrogen bonding between a three-degree amine's nitrogen moiety and the -C-OH bond is another interaction that can demonstrate the nature of adsorption. **Figure 3-4-8 (a)** further illustrates the potential π-π interaction between the MAC@Al surface and the aromatic moiety of crystal violet dye. **Figure 3-4-8 (b)** shows the after-CV adsorption EDS analysis of the adsorbent, confirming the removal of dyes from wastewater. Freundlich adsorption is more practical when crystal violet dye is present on the MAC@Al surface in nature, according to isotherm studies like Langmuir and Freundlich. Increased anionic surface characteristics of the MAC@Al adsorbent and decreased repulsion of the cationic crystal violet dye are the causes of the improved adsorption at higher dye pH. Thus, the increased adsorptive efficacy of CV dye at higher pH is demonstrated by the pHzpc investigation**. Figure 3-3 (a, c, e, g and i) and Figure 3-1 (3.3)** are depicted as XPS and SEM analysis confirming the adsorption of CV dye onto the surface of MAC@Al. from SEM image it is clear the porous structure of the adsorbent gets changed after CV dye adsorption and from XPS analysis it is showing the nitrogen on the surface of the adsorbent making it sensible for adsorption of CV dye.

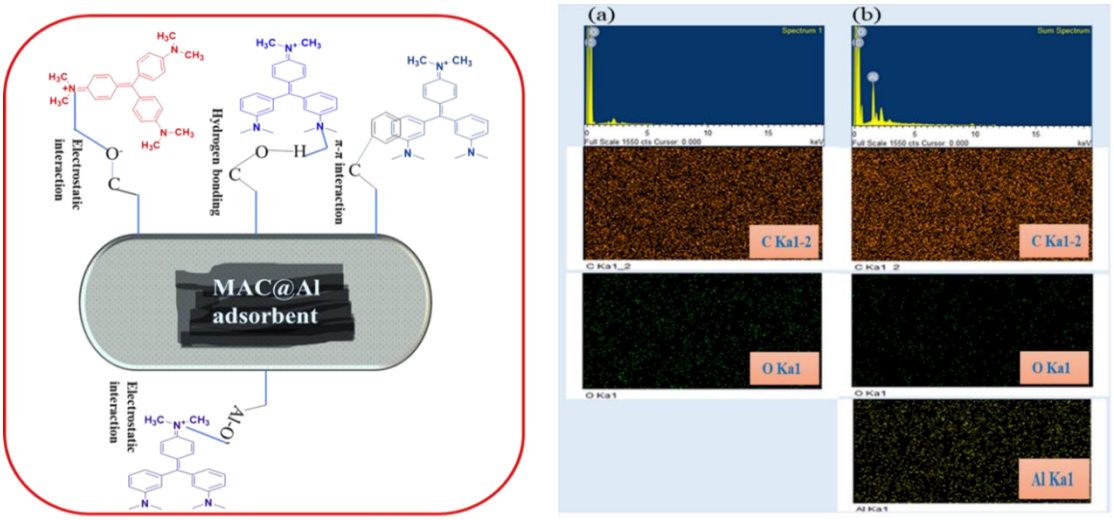

Figure 3-4-8 (a) The proposed mechanism representation in case of crystal violet dye adsorption on the MAC@Al adsorbent surface, **(b)** EDS analysis after adsorption of CV dye on MAC@Al.